STEM CELLS TRANSLATIONAL MEDICINE®

TISSUE ENGINEERING AND REGENERATIVE MEDICINE

Delivery of Differentiation Factors by Mesoporous Silica Particles Assists Advanced Differentiation of Transplanted Murine Embryonic Stem Cells

ALFONSO E. GARCIA-BENNETT,[a,b,*] MARIYA KOZHEVNIKOVA,[c,*] NICLAS KÖNIG,[c,*] CHUNFANG ZHOU,[b] RICHARDSON LEAO,[c] THOMAS KNÖPFEL,[d] STANISLAVA PANKRATOVA,[e] CARL TROLLE,[c] VLADIMIR BEREZIN,[e] ELISABETH BOCK,[e] HÅKAN ALDSKOGIUS,[c] ELENA N. KOZLOVA[c]

Key Words. Cell transplantation • Differentiation • Embryonic stem cells • Nervous system • Neural differentiation • Neural stem cell • Stem cell culture • Transplantation

ABSTRACT

Stem cell transplantation holds great hope for the replacement of damaged cells in the nervous system. However, poor long-term survival after transplantation and insufficiently robust differentiation of stem cells into specialized cell types in vivo remain major obstacles for clinical application. Here, we report the development of a novel technological approach for the local delivery of exogenous trophic factor mimetics to transplanted cells using specifically designed silica nanoporous particles. We demonstrated that delivering Cintrofin and Gliafin, established peptide mimetics of the ciliary neurotrophic factor and glial cell line-derived neurotrophic factor, respectively, with these particles enabled not only robust functional differentiation of motor neurons from transplanted embryonic stem cells but also their long-term survival in vivo. We propose that the delivery of growth factors by mesoporous nanoparticles is a potentially versatile and widely applicable strategy for efficient differentiation and functional integration of stem cell derivatives upon transplantation. STEM CELLS TRANSLATIONAL MEDICINE *2013;2:906–915*

[a]Nanotechnology and Functional Materials, Department of Engineering Sciences, Ångstrom Laboratory, Uppsala University, Uppsala, Sweden; [b]Nanologica AB, Stockholm, Sweden; [c]Department of Neuroscience, Uppsala University Biomedical Center, Uppsala, Sweden; [d]RIKEN Brain Science Institute, Saitama, Japan; [e]Protein Laboratory, Department of Neuroscience and Pharmacology, Panum Institute, Copenhagen University, Copenhagen, Denmark

[*]Contributed equally as first authors.

Correspondence: Elena Kozlova, Ph.D., Department of Neuroscience, Uppsala University Biomedical Center, Box 593, SE-751 24 Uppsala, Sweden. Telephone: 46-18-471-49-68; Fax: 46-18-51-15-40; E-Mail: elena.kozlova@neuro.uu.se; or Alfonso Garcia-Bennett, Ph.D., Department of Materials and Environmental Chemistry, MMK, Arrhenius Laboratory, Stockholm University, S-106 91 Stockholm, Sweden. Telephone: 0046-(0)733865151; E-Mail: alfonso@mmk.su.se

Received April 9, 2013; accepted for publication June 6, 2013; first published online in SCTM *EXPRESS* October 2, 2013.

1066-5099/2013/$20.00/0

http://dx.doi.org/10.5966/sctm.2013-0072

INTRODUCTION

Degeneration of motor neurons (MNs) is a hallmark of devastating diseases such as amyotrophic lateral sclerosis and spinal muscular atrophy, but it is also a serious consequence of spinal cord injuries. One attractive future treatment option for these conditions is to replace the lost MNs with stem cell-derived MNs [1]. To survive after transplantation, stem cells have to be immature when transplanted but at the same time should be predifferentiated to committed precursor cells that might be able to differentiate and integrate into the appropriate neural circuitry after transplantation. Although generation of MNs in vivo from stem cell populations has been reported [2], their poor survival and the limited differentiation into mature MNs hamper the translational potential of this approach. In vitro, protocols for differentiating embryonic stem cells to MNs are well-established and rely on the use of retinoic acid and either the sonic hedgehog protein or its agonist purmorphamine [3, 4], followed by treatment with neurotrophic factors such as ciliary neurotrophic factor (CNTF) and glial cell line-derived neurotrophic factor (GDNF). Since these differentiation factors will not be present in the adult animal at the site of the transplant, a reliable means of delivering them to the transplanted cells would be of great advantage.

Mesoporous silica particles are attractive as a highly robust and tunable delivery platform. Their use as drug delivery vehicles has resulted in many advances in areas as diverse as pharmaceutical formulation, controlled drug release, and diagnostics [5, 6]. Here, we explored a new potential application of these silica particles, namely as a delivery system for controlled release of differentiation factors to transplanted mouse embryonic stem cell (mESC)-derived MN precursors with the aim to induce their differentiation to functional MNs in situ.

MATERIALS AND METHODS

Synthesis of Mesoporous Silica With 20-nm Pores

The mesoporous silica have been characterized previously [7]. The average particle size for mesoporous silica (Meso) in our work, as measured by dynamic light scattering, is 12 μm. Scanning electron microscopy (SEM) image characterization of the particles is shown in Figure 1A.

Pluronic 123 (4 g; triblock copolymer, $EO_{20}PO_{70}EO_{20}$; Sigma-Aldrich, St. Louis, MO,

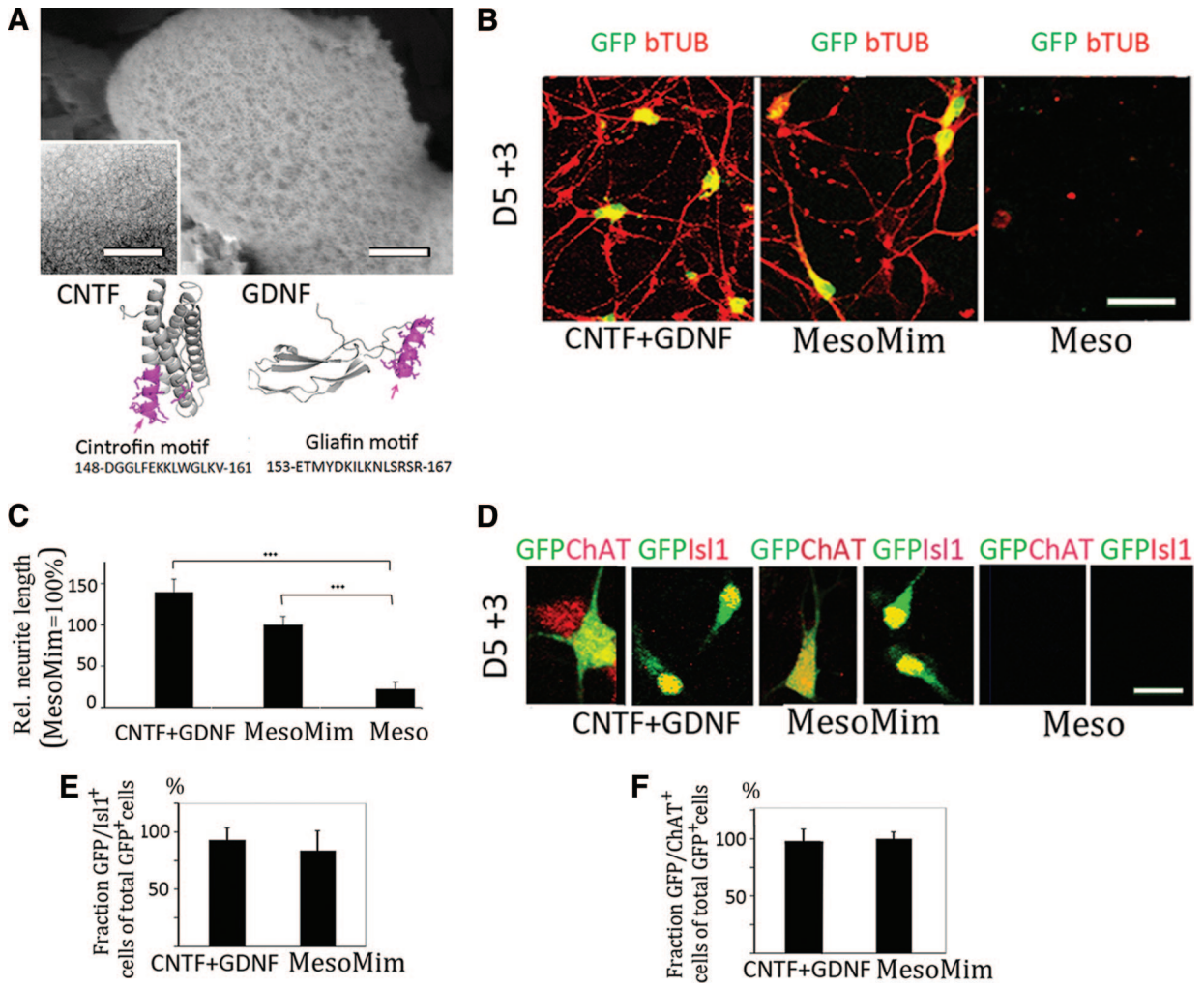

Figure 1. Mesoporous silica loaded with differentiation factors induce motor neuron differentiation in vitro. **(A):** Top: Scanning and transmission (inset) electron micrographs of Meso. Scale bars = 200 nm (main panel) and 50 nm (inset). Bottom: CNTF with the Cintrofin motif shown in magenta and GDNF with the Gliafin motif shown in magenta. Amino acid residues are numbered according to UniProtKB entry nos. P26441 (Cintrofin) and Q07731 (Gliafin). **(B):** Differentiating motor neurons (MNs) extended numerous bTUB-labeled neurites (red) on poly-D-lysine (PDL)/laminin-coated coverslips after direct administration of CNTF and GDNF or treatment with MesoMim. Neurite formation was absent from MN precursors exposed to unloaded Meso. Scale bar = 75 μm. **(C):** Quantitative analysis of neurite length from MNs on PDL/laminin-coated coverslips after direct administration of CNTF and GDNF, treatment with MesoMim, or treatment with unloaded Meso. Results from 7–10 experiments are expressed as mean ± SEM, and the MesoMim group is set at 100%. Direct and MesoMim administration of the factors induced a significantly greater extent of neurite outgrowth compared with the unloaded Meso group; ***, $p < .001$. No statistically significant differences were observed between groups with direct or MesoMim administration of the factors ($p > .05$). **(D):** HB9-GFP$^+$ MNs expressed the MN markers ChAT and Isl1 in a 3-day differentiation assay after treatment with CNTF and GDNF or MesoMim but not in the absence of factors. Scale bar = 25 μm. **(E, F):** Almost all GFP$^+$ cells expressed Isl1 **(E)** and ChAT **(F)** after treatment with CNTF and GDNF or MesoMim. Abbreviations: bTUB, β-tubulin; ChAT, choline acetyltransferase; CNTF, ciliary neurotrophic factor; D, day; GDNF, glial cell line-derived neurotrophic factor; GFP, green fluorescent protein; Isl1, Islet 1; Meso, mesoporous silica; MesoMim, mesoporous silica loaded with peptide mimetics; Rel., relative.

http://www.sigmaaldrich.com) and 3.3 g of trimethyl benzene (Mesitylene; Sigma-Aldrich) were dissolved in 127 ml of distilled H_2O and 20 ml of HCl (37%; Sigma-Aldrich) with stirring at 40°C for 4 hours. After the addition of 9.14 ml of tetraethyl orthosilicate (Sigma-Aldrich) to the solution, the mixture was stirred for an additional 8 minutes at a speed of 500 rpm and aged at 40°C for 24 hours, followed by curing hydrothermal treatment at 100°C for another 24 hours. Finally, the mixture was filtered, washed with distilled water, and dried at room temperature. The removal of the template and swelling agents was performed by calcining the as-synthesized material at 550°C for 6 hours with a heating ramp rate of 1.5°C/minute under a stream of air.

Physical and Chemical Characterization of Mesoporous Silica

The loading amount of peptide was determined by thermogravimetric analyses (described below) (PerkinElmer Life and Analytical Sciences, Waltham, MA, http://www.perkinelmer.com) (supplemental online Fig. 1). Scanning was performed from 20°C to 900°C at a heating rate of 20°C/minute. The plug-in gas atmosphere was dry air (flow rate, 20 ml/minute). The sample weight varied from 5 to 10 mg.

Nitrogen adsorption-desorption isotherm was applied to the calcined mesoporous silica powders for the characterization

of porosity using a Tristar II 3020 apparatus (Micromeritics, Norcross, GA, http://www.micromeritics.com) (supplemental online Fig. 2). Calcined samples were degassed at 300°C for 6 hours under nitrogen gas flow. Factor-loaded samples were degassed at 60°C for 48 hours prior to analysis. The pore size distribution was calculated using density functional theory, assuming cylindrical pore geometry, using the software package included with the Micromeritics instrument.

SEM images were recorded using a LEO 1550 scanning electron microscope equipped with a Schottky field emission gun operated at an accelerating voltage of 1–3 kV and ×20,000 to ×50,000 magnification on samples with no gold coatings (Fig. 1A). The SEM images were obtained using a JSM-7401F (JEOL, Tokyo, Japan, http://www.jeol.com/en/) operating at 0.5–2 kV with no gold coating.

Transmission electron microscopy of the calcined samples (Fig. 1A, inset) was conducted with a JEOL-3010 (JEOL) microscope operating at 300 kV (Cs, 0.6 mm; 1.7 Å resolution). Images were recorded using a charge-coupled device camera (Keen View, SIS Analysis Specialized Imaging; Olympus Soft Imaging Solutions, Münster, Germany, http://www.olympus-global.com; 1,024 × 1,024 pixels; 23.5 × 23.5 μm field of view) at ×30,000 to ×100,000 magnification using low-dose conditions on as-synthesized and calcined samples.

Synthesis of Peptide Mimetics

The peptides Cintrofin and Gliafin, derived from the ciliary neurotrophic factor (148-DGGLFEKKLWGLKV-161; UniProtKB entry no. P26441) and glial cell line-derived neurotrophic factor (153-ETMYDKILKNLSRSR-167; UniProtKB entry no. Q07731), respectively, were synthesized using the solid-phase Fmoc protection strategy, and purity was estimated to be at least 80% by high-performance liquid chromatography. All of the peptides were synthesized by Schafer-N AS (Copenhagen, Denmark, http://www.schafer-n.com) as dendrimers composed of four monomers coupled to a lysine backbone. During the synthesis of biotinylated peptides, only N-terminal amino acids were biotin-labeled amino acids. Thus, each tetrameric dendrimer contained four biotin residues.

Loading and Release of Peptide Mimetics Gliafin and Cintrofin

The peptide mimetics were loaded via impregnation in water. Meso samples (50 mg) were added to 0.5 ml of Gliafin in a water solution at a concentration of 8.87 mg/ml and stirred at 4°C for 16 hours. Meso samples (25 mg) were added to a 0.4-ml Cintrofin water solution at a concentration of 4.4 mg/ml and stirred at 4°C for 16 hours. The water in both solutions was evaporated under atmospheric conditions. The loading amount of peptide was determined by thermogravimetric analysis (PerkinElmer). Scanning was performed from 20°C to 900°C at a heating rate of 20°C/minute. The plug-in gas atmosphere was dry air (flow rate, 20 ml/minute). The sample weights varied from 5 to 10 mg. Loading efficiencies of mesopores were 8.3 and 11.8 wt% for Cintrofin and Gliafin, respectively (supplemental online Fig. 1A). Accordingly, adsorption isotherm data showed a considerable reduction in the pore volume and pore size of the mesoporous silica because of the incorporation of mimetics within the mesopores (supplemental online Fig. 2). Powder x-ray diffractograms of loaded samples revealed that the peptides were loaded in an amorphous state, as diffraction peaks were not observed. Biotinylated versions of the peptide mimetics were loaded in a similar manner as described above. To study the release kinetics, the 25 mg of peptide-loaded mesoporous silica particles were incubated in a conical tube containing 2 ml of simulated body fluid (SBF) [8] at 37°C under continuous gentle shaking (30 rpm). Small samples taken at certain times were centrifuged for 10 minutes at 10,000 rpm, and the amount of peptide released was quantified at 205 nm using a Spectronic 1001 (Bie & Berntsen, VWR, Rødovre, Denmark, https://dk.vwr.com) (supplemental online Fig. 1B). After each sampling, an equal volume of SBF was added to the tube.

Cell Culture

We used an mESC line carrying a transgenic reporter gene in which expression of the green fluorescent protein (GFP) is driven by promoter element from the *Hb9* gene (*Hb9::GFP*) The cells were cultured according to a previously published protocol with minor modifications [2].

To differentiate mESCs into spinal MNs in vitro, embryonic stem cell (ESC) colonies were partially dissociated after 2 days and plated at 100,000 cells per milliliter on ultralow-attachment six-well plates (Corning, Inc., Corning, NY, http://www.corning.com) with ADFNB medium (Advanced Dulbecco's modified Eagle's medium/F12:Neurobasal [1:1], 1× GlutaMAX supplement [Invitrogen, Carlsbad, CA, http://www.invitrogen.com], 1× B27 supplement [Invitrogen], 1× N2 supplement [Invitrogen], 0.1 mM 2-mercaptoethanol [Sigma-Aldrich], and 1× penicillin/streptomycin) to form embryoid bodies (EBs). EBs were split 1:4 on day 2, and the medium was supplemented with 0.1 μM all-trans retinoic acid (Sigma-Aldrich) and 0.5 μM purmorphamine (Calbiochem, San Diego, CA, http://www.emdbiosciences.com). EBs were cultured for an additional 3–4 days when approximately 20% of the cells expressed GFP and were then placed in differentiation assay or transplanted to adult *nu/nu* mice (described below, under Surgery and Transplantation).

For the in vitro differentiation assay and electrophysiological analysis, EBs were dissociated using TrypLE Express (Invitrogen) on day 5 and plated on poly-L-ornithine- and mouse laminin (Sigma-Aldrich)-precoated coverslips in ADFNB medium supplemented with GDNF (10 ng/ml; Upstate Biotechnology, Lake Placid, NY, USA) and CNTF (10 ng/ml; Upstate Biotechnology) or with Meso Cintrofin (1 μM) and Meso Gliafin (1 μM) (nonbiotinylated and biotinylated) and cultured for an additional 2–3 days.

Surgery and Transplantation

On the day of transplantation, 8–12 EBs to be transferred to each individual dorsal root ganglion (DRG) cavity were collected from transfected (i.e., with VSFP2.42; described below) and nontransfected cultures into Eppendorf tubes that contained neurosphere culture medium. Adult male NMRI (Naval Medical Research Institute) *nu*/*nu* mice (25–30 g body weight; Möllegaard and Bomholtgard Breeding and Research Centre, M&B A/S, Bomholt, Denmark, http://www.taconic.com) were anesthetized with an intraperitoneal injection of xylazine (Rompun veterinary; Bayer Animal Health, Leverkusen, Germany, http://www.animalhealth.bayer.com) and ketamine (Ketaminol Vet; Intervet International B.V., Boxmeer, The Netherlands, http://www.merck-animal-health.com; 10 and 100 ng/g body weight, respectively) prior to surgery. The lower lumbar vertebral column was exposed via a midline incision in the skin and fascia and the left L4

Table 1. Antibodies used for immunohistochemistry

Antigen/label	Host	Catalog no.	Source	Dilution
β-Tubulin	Mouse	32-2600	Invitrogen	1:500
ChAT	Goat	AB144P	Millipore	1:200
Islet1	Mouse	40.3A4	DSHB	1:200
Cy3-streptavidin		016-160-084	Jackson Immunoresearch	1:1,000
AMCA	Donkey anti-rabbit	711-155-152	Jackson Immunoresearch	1:100
Cy3	Donkey anti-mouse	715-165-151	Jackson Immunoresearch	1:500
Texas Red	Goat anti-mouse	T862	Invitrogen	1:200

Manufacturers: Developmental Studies Hybridoma Bank (DSHB), Iowa City, IA, http://www.uiowa.edu/~dshbwww; Invitrogen, Carlsbad, CA, http://www.invitrogen.com; Jackson Immunoresearch Laboratories, West Grove, PA, http://www.jacksonimmuno.com; Millipore, Billerica, MA, http://www.millipore.com.
Abbreviation: ChAT, choline acetyltransferase.

and L5 DRGs were exposed via partial laminectomy. The dorsal roots were cut just proximal and distal to the ganglia, and the ganglia were carefully removed, leaving the ventral roots intact. During the removal of the DRGs, the small dorsal ramus of the spinal nerve, which arises just distal to the DRG, was interrupted.

The EBs were placed into the DRG cavities on the top of the ventral root. Mesoporous particles that contained 1.2 μg of Cintrofin and 1.2 μg of Gliafin or unloaded mesoporous particles were placed on top of the transplant. To study the interactions between MesoMim (mesoporous silica loaded with peptide mimetics of CNTF and GDNF) that contained biotin-labeled mimetics and differentiating HB9-GFP motor neurons, they were placed in a similar manner on the transplanted EBs in one set of animals or in addition on another side of the DRG cavity in another set of the animals. The dorsal root was attached to the EBs, and the muscles and skin were closed in layers. Survival periods were 3, 7, 10, and 14 days for the biotinylated MesoMim experiments ($n = 12$), and 2 weeks ($n = 27$) or 2 months ($n = 24$) for morphological and electrophysiological analysis of the transplants. At the appropriate survival time, recipient mice were reanesthetized and perfused via the left ventricle with saline (approximately 38°C) followed by a fixative solution that contained 4% formaldehyde (vol/vol) and 14% saturated picric acid (wt/vol) in phosphate-buffered saline (PBS; approximately 4°C, pH 7.35–7.45) for morphological analysis of the transplants, or dissected unfixed to harvest transplants for electrophysiology.

Immunohistochemistry

Cultures

Cells cultured on coverslips were fixed with 4% paraformaldehyde, permeabilized with 0.1% Triton X-100 and 10% donkey serum blocking solution in PBS, and incubated with primary antibodies overnight and secondary antibodies for 4 hours at room temperature.

Transplants

The DRG area with the transplant and attached dorsal root and spinal nerve were removed from fixed mice, postfixed at 4°C for 4 hours, and cryoprotected overnight in PBS containing 15% sucrose. Serial sections (12 μm) were cut through the transplant on a cryostat, and placed on SuperFrost-Plus glass slides (Menzel-Gläser, Braunschweig, Germany, http://www.menzel.de). Sections and coverslips were preincubated with blocking solution (1% bovine serum albumin, 0.3% Triton X-100, and 0.1% NaN_3 in PBS) for 1 hour at room temperature and then incubated overnight at 4°C with primary antibodies (Table 1). After being washed with PBS, sections were incubated with secondary antibodies (Table 1). To control for unspecific labeling, sections were processed without incubation with primary antibodies.

To visualize biotinylated peptide mimetics, sections were incubated with Cy3-conjugated streptavidin for 4 hours at room temperature. Sections were rinsed in PBS and mounted using 2% *N*-propyl gallate in 50% glycerol in PBS.

Microscopy

Immunolabeled cultures and sections were analyzed under a Nikon Eclipse E800 fluorescence microscope (Nikon, Tokyo, Japan, http://www.nikon.com). For photography, a Nikon DXM1200F digital camera system was used. Fluorescent stainings were also analyzed by confocal microscopy using a Zeiss LSM 510 META system (Carl Zeiss, Oberkochen, Germany, http://www.zeiss.com). Captured images were auto-leveled using Adobe Photoshop software (Adobe Systems Inc., San Jose, CA, http://www.adobe.com). To study the interrelations between biotinylated mimetics and transplanted stem cells, images were acquired with a Zeiss LSM 510 Meta confocal microscope and $\times$63/1.4 NA plan-apochromate lens. *z*-Stacks were acquired with an optical slice thickness of 0.8 μm and interval of 0.5 μm.

The average length (in vitro and in vivo) of neuronal processes per cell (the proportion of neurite intersections per nerve cell body) was estimated using a software package, ProcessLength, developed at the Protein Laboratory (Copenhagen, Denmark) [9]. For the evaluation of 2-week and 2-month transplant volumes, images from each slide (every sixth section) were taken through the whole transplant, and enhanced green fluorescent protein (EGFP)-positive areas and transplant volumes were calculated using NIH ImageJ software (http://rsb.info.nih.gov/ij). The transplant volume was calculated according to the formula $A = TK[\sum(S_1 \text{ to } S_n)]$, in which T is the thickness of the section ($T = 12$ μm), K is the number of sections between the measured areas ($K = 6$), and S is the area of the transplant on the sections from 1 to n.

Electrophysiology

At the end of the differentiation assay, the cultures were transferred to the stage of an upright microscope and perfused with artificial cerebrospinal fluid (aCSF) plus HEPES buffer (119 mM NaCl, 26 mM $NaHCO_3$, 10 mM glucose, 2.5 mM KCl, 1 mM NaH_2PO_4, 1.5 mM $MgSO_4$, 1.5 mM $CaCl_2$, and 10 mM HEPES). For current-clamp recordings, glass pipettes were filled with potassium gluconate internal solution (17.5 mM KCl, 122.5 mM potassium gluconate, 9 mM NaCl, 1 mM $MgCl_2$, 3 mM Mg-ATP, 0.3 mM GTP-Tris, 1 mM HEPES, and 0.2 mM EGTA). The pipettes had resistances that ranged from 4 to 6 MΩ. Only recordings with $<$15 MΩ series resistance were used for the analysis. The data were

acquired using a patch-clamp amplifier (Multiclamp 700B; Molecular Devices, Sunnyvale, CA, http://www.moleculardevices.com), low-pass filtered at 10 kHz, and digitized at 20 KHz using WinWCP (Dr. John Dempster, Strathclyde University, Glasgow, U.K.). De- and hyperpolarizing currents were injected with 50-pA increments from −50 pA to 300 pA.

Voltage-Sensitive Fluorescent Protein Imaging

For voltage-sensitive fluorescent protein (VSFP) imaging, MN precursors were electroporated before transplantation with a plasmid that carried the voltage sensitive reporter protein VSFP2.42 under a constitutively active, cytomegalovirus early enhancer/modified chicken β-actin hybrid promoter [10] using an a Nucleofector (Lonza, Walkersville, MD, http://www.lonza.com) according to the manufacturer's instructions for the Optimal Nucleofector Program A33. Nontransfected explants served as a control. Two weeks or 2 months after transplantation, the animals were reanesthetized, the site of surgery was exposed, and the transplants were removed, incubated for 10 minutes in aCSF, and then placed into a microincubator where EGFP-positive cells were identified and taken for the analysis of VSFP2.42-reported voltage signals.

For imaging, the transplants were removed from live animals and cut on a vibratome with 200-μm slices, which were transferred to the stage of an upright microscope and continuously perfused with aCSF with no HEPES equilibrated with 95% O_2 + 5% CO_2. Excitation was provided by a light-emitting diode array [11]. For VSFP2.42 imaging, excitation was centered at 520 nm, and a 605 nm low-pass filter was used for emission, thus avoiding cross-talk from EGFP fluorescence emission. Image series were acquired using a 16×, 0.8 NA objective (Nikon), custom-made software, and scientific complementary metal oxide semiconductor camera (Andor Belfast, U.K., http://www.andor.com) using rates between 25 and 100 frames per second. To detect active neurons, we bath-applied 10 μM carbachol to elicit action potentials in differentiated neurons while monitoring changes in VSFP fluorescence caused by action potential firing [10].

Statistics

The data were analyzed using one-way repeated-measures analysis of variance followed by the Bonferroni post hoc test using Prism version 4.02 software (GraphPad Software, Inc., San Diego, CA, http://www.graphpad.com).

RESULTS

Functionalized Mesoporous Silica Particles Are Suitable for Induction of MN Precursor Differentiation In Vitro

Predifferentiated MN precursors can be transplanted to the nervous system to continue their differentiation and incorporation into local neural circuits in situ, if they are supplied with the appropriate neurotrophic factors, such as CNTF and GDNF [2, 4, 12, 13]. The goal of the present study was to develop a vehicle for the delivery of these differentiation factors in vivo to transplanted ESC-derived MN precursors to achieve their functional differentiation after transplantation.

We first tested whether we could induce differentiation of MNs in vitro from predifferentiated MN precursors by delivering differentiation factors by means of mesoporous particles (Fig. 1). We used silica with an enlarged pore size (Meso) in order to enable encapsulation of the peptides Cintrofin and Gliafin (Fig. 1). These are established mimetics (Mim) of the neurotrophic factors CNTF and GDNF, respectively [12, 13]. Cintrofin has been shown to induce neuronal differentiation and promote survival by binding to the leukemia inhibitory factor receptor and common cytokine receptor chain gp130 [14]. Gliafin contains a sequence motif that was identified as a GDNF binding site for the neural cell adhesion molecule and that is capable of inducing neurite outgrowth [15].

MN precursors responded similarly to direct treatment with CNTF and GDNF or to delivery of Cintrofin and Gliafin by silica with regard to the neuritogenic response (Fig. 1B, 1C, $p < .001$) and the expression of the MN markers choline acetyltransferase (ChAT) (Fig. 1D, 1F) and Islet 1 (Isl1) (Fig. 1D, 1E). No expression of ChAT or Isl1 and almost no neurite outgrowth from HB9-GFP$^+$ cells was observed in cultures treated with unloaded Meso (Fig. 1A–1D). No labeling was observed after omission of primary antibodies.

To determine the relationship between differentiating MNs and mimetics, Cintrofin and Gliafin were labeled with biotin prior to their loading into silica (Materials and Methods). The cultures were fixed and incubated with Cy3-conjugated streptavidin to visualize the peptide mimetics. In confocal microscopy, biotinylated mimetics were observed as small clusters of different sizes on the surface of differentiating MN cell bodies as well as along their neurites (supplemental online Fig. 3), indicating that the differentiating cells had sufficient access to the growth factors during the duration of the differentiation assay.

MNs Induced by Peptide-Loaded Mesoporous Silica Display Electrophysiological Properties of Mature MNs

As shown above, we were able to achieve morphological differentiation of MN precursors in vitro with mimetics delivered by Meso. We next investigated the physiological properties of these MNs. At the end of the differentiation assay, the coverslips were transferred to a recording chamber on a patch-clamp setup (supplemental online Fig. 4). Targeted patch-clamp recordings revealed that HB9-GFP$^+$ cells, predifferentiated in culture with differentiation factors delivered by loaded silica particles, displayed a resting membrane potential close to the physiological range and could be driven to high spiking frequencies (supplemental online Fig. 4). This behavior was similar to that of cells treated with factors delivered in free form to the cultures. Thus, the delivery of trophic factors in vitro by mesoporous silica induced differentiation of MN precursors to MNs with typical electrophysiological properties (Fig. 2A).

Cotransplantation with Mesoporous Particles Loaded with Mimetics Allows Efficient Generation of MNs In Vivo

We next investigated whether the use of mesoporous particles loaded with mimetics is beneficial for the survival and differentiation of transplanted MN precursors in vivo. Predifferentiated EBs were placed into the DRG cavity of adult mice. We have previously used the DRG cavity in several stem cell transplantation experiments [16–18]. It is an attractive site for transplantation because the transplant is easily identified and no other neurons reside in the cavity after removal of the DRG. It thus makes transplantation to the DRG cavity a useful experimental model and a valuable intermediate step in translating in vitro protocols to in vivo applications.

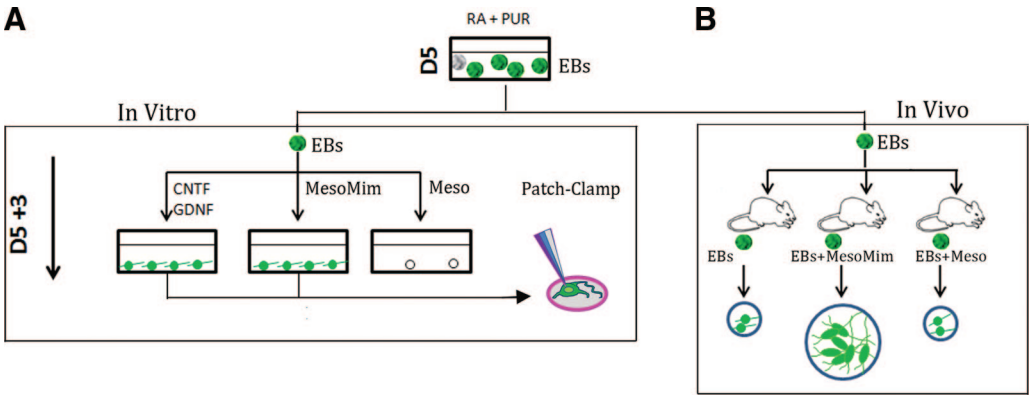

Figure 2. Experimental setup and schematic presentation of the main results on the efficacy of Meso as a peptide mimetic delivery system for the generation of functional motor neurons (MNs). **(A):** In vitro. After 5 days of treatment of the embryonic stem cells with RA+PUR in vitro, EBs were dissociated and treated for the next 3 days with direct incubation of CNTF and GDNF, Meso loaded with the CNTF and GDNF peptide mimetics Cintrofin and Gliafin (MesoMim), or unloaded Meso. Cultures treated with CNTF/GDNF or MesoMim differentiated into mature MNs, whereas only occasional cells survived without treatment (Meso). Patch-clamp analysis confirmed the functionality of neurons generated with trophic factors delivered in free form and with Meso. **(B):** In vivo. Shown are the experimental setup and main results of the efficacy of MesoMim as a delivery system for the generation of functional MNs in vivo. Transfected EBs were transplanted to the dorsal root ganglion cavity of nu/nu mice. Transplants were untreated control (EBs), treated with MesoMim (EBs+MesoMim), or control with unloaded Meso (EBs+Meso). Treatment with MesoMim resulted in increased transplant volumes and neurite growth compared with the control groups. Abbreviations: CNTF, ciliary neurotrophic factor; D, day; EB, embryoid body; GDNF, glial cell line-derived neurotrophic factor; Meso, mesoporous silica; MesoMim, mesoporous silica loaded with peptide mimetics; PUR, purmorphamine; RA, retinoic acid.

EBs were implanted in the following combinations: (a) EBs alone, (b) EBs with MesoMim, and (c) EBs with unloaded Meso. Some EBs from the first and second groups were transfected with VSFP2.42 for subsequent electrophysiological analysis [10, 11].

After 2 weeks, neurons in MesoMim-treated transplants displayed extensive neurite outgrowth and expressed ChAT (Fig. 3A, left, 3D). Neurons in control transplants (EBs and EBs+Meso) remained small, with minimal neurite outgrowth and no ChAT expression (Fig. 3B, left). The volume of MesoMim-treated transplants was almost 10 times as large as in the control groups (Fig. 3C, left).

After 2 months, MNs in MesoMim-containing transplants displayed extensive neurite arborizations and prominent ChAT expression (Fig. 3A, right), in contrast to control transplants, where only occasional neurons were detected, and all of these displayed minimal neurite outgrowth (Fig. 3B, right). Relative transplant volumes were significantly larger in the MesoMim-treated group compared with the control groups (Fig. 3C, right; $*$, $p < .05$). No statistically significant differences were observed between the EBs and EBs+Meso groups ($p > .05$). Relative axonal extensions within the transplant were significantly larger in the MesoMim-treated group compared with the control groups (Fig. 3D, right; $*$, $p < .05$, $**$, $p < .01$). No statistically significant differences were observed between the EBs and EBs+Meso groups ($p > .05$). Furthermore, we detected neurite extensions in the dorsal roots and in the dorsal rami of the spinal nerve associated with the transplant only in the MesoMim-treated transplants (not shown). Taken together, cotransplantation of EBs with MesoMim resulted in increased transplant size, as well as improved survival and induction of robust neurite outgrowth from differentiated MNs (Fig. 2B).

We asked how long the mimetics were available to the cells and whether they attracted the growing neurites from the differentiating MNs in the transplants. To detect any possible trophic effect, MesoMim-containing biotinylated mimetics were implanted together with EBs in the DRG cavity and also at the caudal pole of the transplant. The transplants were collected 3, 7, 10, and 14 days after transplantation, and the presence of the mimetics was visualized with Cy3-conjugated streptavidin. A reduction in the amount of labeled mimetics in the area of the transplant occurred between days 3 and 10 (supplemental online Fig. 5). The distribution of the mimetics was dispersed throughout the graft area, but always in close association with the differentiating MN cell bodies and their outgrowing neurites (Fig. 4A, left). Extensive neurite growth was observed toward the caudally placed MesoMim implant, which displayed high levels of labeled mimetics (Fig. 4A, right), suggesting the presence of a trophic gradient of MesoMim radiating outward from the caudal implant site. As described above, neurite outgrowth from EBs (Fig. 3B, left) or EBs treated with MesoMim (Fig. 3A, left), but without MesoMim in the caudal pole of the DRG cavity, did not result in directed growth of transplanted cells (Fig. 3B, left).

To assess the physiological state of the transplants, we used an VSFP imaging approach [19]. Transplants with EBs transfected with a VSFP-expressing construct before transplantation (as described in Materials and Methods) were used for optical membrane potential recordings. The capability of ESC-derived MNs to generate action potentials was assessed at 2 weeks and 2 months post-transplantation (Fig. 4B, 4C). In both untreated (EBs; Fig. 4B) and treated (EBs+MesoMim; Fig. 4C) groups, the cells exhibited action potential firing, demonstrating their physiological functionality.

Discussion

The goal of this study was to demonstrate that a mesoporous silica vehicle can be used for in vivo delivery of differentiation factors to support survival and specific differentiation of transplanted ESC-derived neural progenitors. The use of ordered mesoporous inorganic particles with silica compositions to deliver pharmaceutically active compounds has previously been explored and has resulted in many advances in areas such as pharmaceutical drug formulation, controlled drug release, and

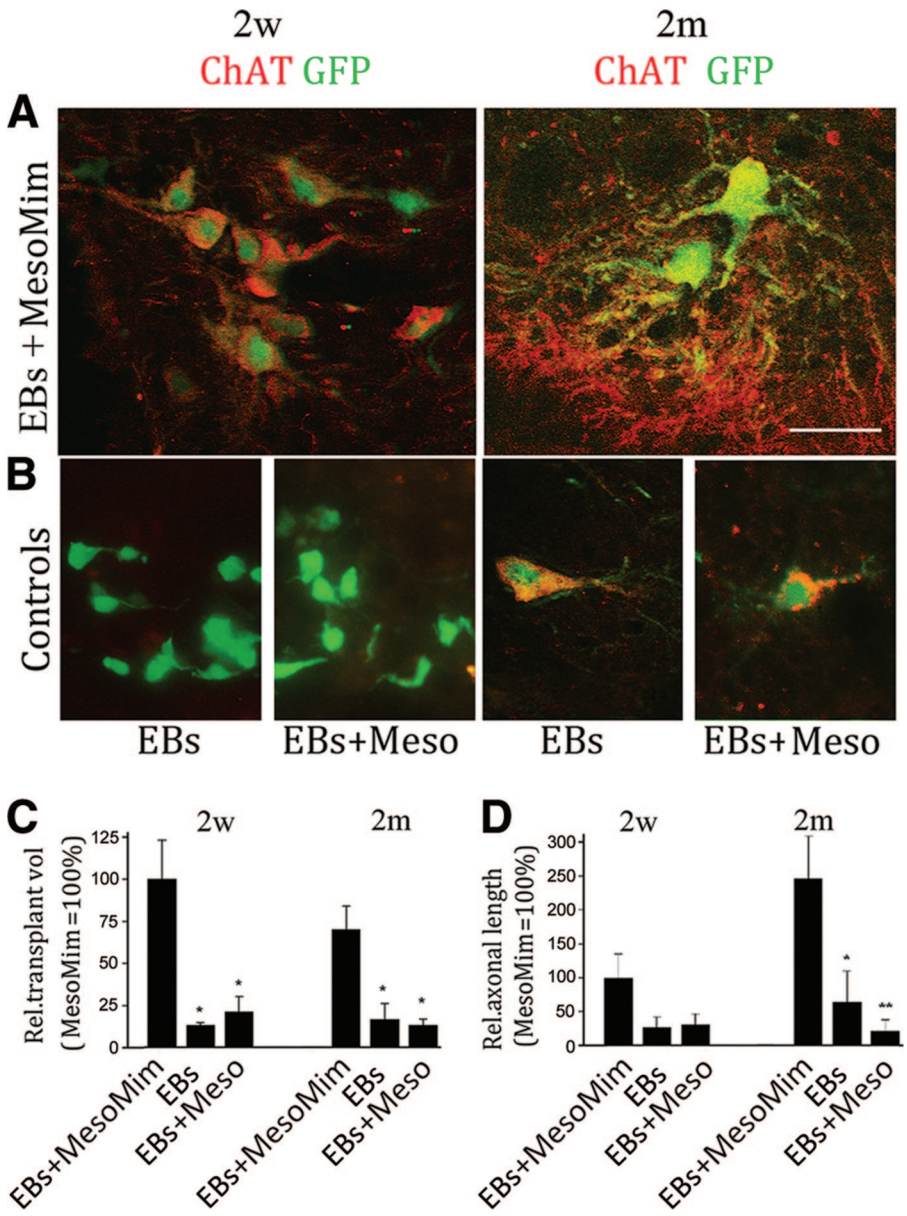

Figure 3. Motor neuron differentiation in transplants induced by MesoMim. **(A, B):** HB9-GFP$^+$ motor neurons (MNs) 2 weeks (left) and 2 months (right) after transplantation of EBs to the dorsal root ganglion cavity with MesoMim **(A)** and EBs alone or cotransplanted with unloaded Meso (controls) **(B)**. After 2 weeks (**[A]**, left), neurons in MesoMim-treated transplants were large, displayed extensive neurite outgrowth, and expressed ChAT, whereas neurons in control transplants (**[B]**, EBs and EBs+Meso) remained small, with minimal neurite outgrowth and no ChAT expression. At 2 months, MNs in mimetic-treated transplants displayed even greater neurite outgrowth and ChAT expression (**[A]**, right) in contrast to control transplants (**[B]**, right) that displayed only scattered ChAT$^+$ neurons with limited neurite outgrowth. Scale bar = 50 μm. **(C):** Relative transplant volumes at 2 weeks and 2 months after the transplantation of EBs together with MesoMim, without Meso (EBs), or with unloaded Meso (EBs+Meso). The results from four to six experiments are expressed as the mean $\pm$ SEM, and the MesoMim group with 2-week transplants is set as 100%. Relative transplant volumes in the MesoMim group were significantly larger compared with controls 2 weeks and 2 months after transplantation. No statistically significant differences were observed between the EB and EBs+Meso groups ($p > .05$): $*$, $p < .05$. **(D):** Relative axonal lengths in the 2-week and 2-month transplants. The results from four to six experiments are expressed as the mean $\pm$ SEM, and the MesoMim group with 2-week transplants is set at 100%. Relative axonal extensions were significantly longer in the MesoMim-treated group compared with the untreated group (EBs) and the group treated with unloaded Meso 2 weeks and 2 months after transplantation. No statistically significant differences were observed between the EB and EBs+Meso groups ($p > .05$): $*$, $p < .05$; $**$, $p < .01$. Abbreviations: ChAT, choline acetyltransferase; EB, embryoid body; GFP, green fluorescent protein; m, months; Meso, mesoporous silica; MesoMim, mesoporous silica loaded with peptide mimetics; Rel., relative; w, weeks.

cell-targeted delivery [5, 20, 21]. Silica mesoporous particles offer novel strategies to encapsulate chemical compounds regardless of their polarity, thereby improving their pharmacokinetic properties without increasing their toxicological profile. Of immediate practical value is the ability of these delivery vehicles to release poorly soluble chemical compounds that had been loaded in the noncrystalline state within their internal pore spaces, thereby significantly enhancing their aqueous solubility profiles and bioavailability [7, 22]. The potential to conjugate specific receptor-targeting groups on the external surface of the

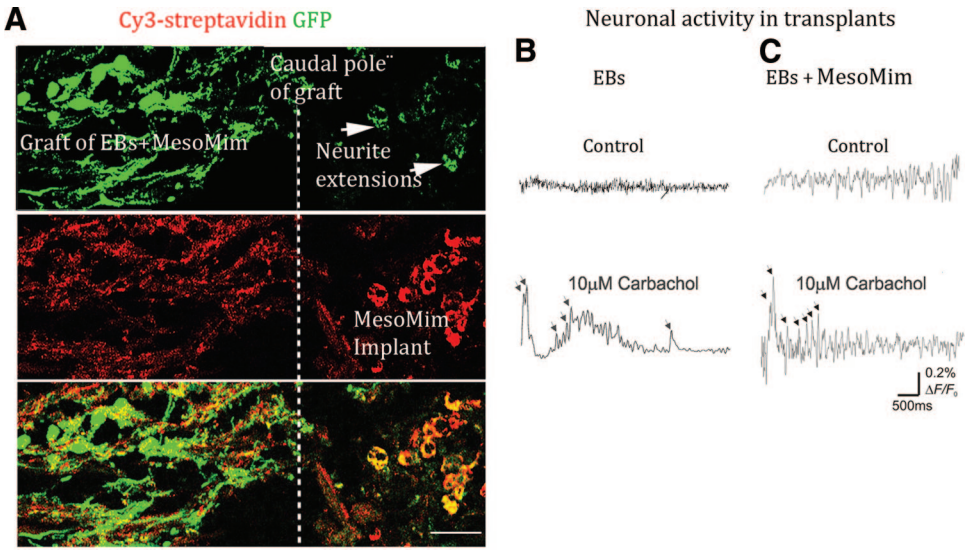

Figure 4. Peptide mimetics assist functional motor neuron differentiation and neurite growth in transplants. **(A):** Localization of peptide mimetics during motor neuron (MN) differentiation 7 days after the transplantation of EBs together with MesoMim (left). MesoMim was also placed distal to the caudal pole of the graft (right). Cy3-streptavidin-labeled mimetics were dispersed throughout the graft site between HB9-GFP$^+$ MN cell bodies and their neurites. Distal to the caudal pole of the graft site, mimetics were highly concentrated in spherical formations, which were closely associated with MN neurites that extended from the graft (arrows). Scale bar = 50 μm. **(B, C):** Carbachol-induced electrical activity in VSFP2.42-expressing 2-month-old transplants that were untreated **(B)** and treated with MesoMim **(C)** under control conditions and after the application of 10 μM carbachol. The arrows show fluorescence changes induced by action potentials in both types of transplants. Abbreviations: EB, embryoid body; GFP, green fluorescent protein; Meso, mesoporous silica; MesoMim, mesoporous silica loaded with peptide mimetics; MN, motor neuron.

particles and their large internal pore volumes, which may accommodate various chemical compounds, including fluorophores and other nanomaterials, offer a versatile platform for designing multifunctional therapeutic and diagnostic devices. Silica particles possess a pH-dependent solubility and can be dissolved forming silicic acid. The dissolution of the particles in vivo is slow [7] and when applied subcutaneously they disappear only in 3 months, whereas after implantation into the sciatic nerve, the particles disappear much faster [23]. Since our transplants are located in the DRG cavity on the top of the sciatic nerve the elimination of particles is likely to be analogous to their implantation into the sciatic nerve. Alternatively, the particles can be taken up by macrophages. Previous studies have shown significant and rapid uptake of silica particles via active mechanisms into human macrophages with no impairment of macrophage function [6, 24]. Toxicological data from in vitro and in vivo studies suggest that, within the dose ranges envisaged for pharmaceutical and clinical applications, mesoporous materials have no observable harmful effects, are well tolerated, and may even have a positive immunostimulatory effect [6, 20–22].

So far, mesoporous silica or other nanomaterials have not been used as a delivery system for differentiation factors to guide stem cell differentiation. For our study we selected mesoporous materials as carriers because of their easily controlled ordered porous structure, which makes it possible to design and prepare pores of an exact size range in order to load the relevant peptide mimetics and provide for their slow kinetic release. Although other porous silica materials exist, they possess broader pore size distributions that will not contribute to peptide loading. Furthermore, synthetic amorphous silica is already approved as a food additive (E551 under E.U. regulations) and described in the pharmacopeia.

This delivery of differentiation factors can be particularly important for the transplantation to the nervous system, since nerve cells have to be transplanted in an immature stage and require further guidance in vivo to ensure their specific differentiation and incorporation into local neural circuitries. To deliver differentiating factors with pumps or injections is laborious and likely to result in a more diffuse distribution than delivery via nanoparticles that can be placed very close to or even right next to the transplanted cells. Altering pore sizes and other physical properties of mesoporous silica may even permit the sequential delivery of trophic factors with defined concentrations locally to the differentiating stem cells, thereby allowing a more direct transfer of in vitro differentiation protocols to in vivo applications. This method can be also applied to promote neurogenesis and directed differentiation of endogenous neural stem cells. It was not possible, however, to study this aspect in this model, since all DRG neurons were removed. An additional asset of such a vehicle is its applicability in vitro since controlled long-term release of differentiating factors from the mesoporous silica may eliminate the need for repeated administration of these factors in their free form and, thus, both save time and costs, and reduce the risk of culture contamination.

For MN differentiation in vitro, we used CNTF and GDNF or delivered their mimetics with Meso. Neurite outgrowth and expression of the MN-specific markers ChAT and Isl1 in differentiation assays as well as patch-clamp analysis revealed a similar outcome for both forms of delivery. Confocal images showed close association of cell bodies and growing neurites with labeled peptide mimetics (not shown) during all stages of the in vitro differentiation assay, suggesting that differentiating MN precursors had lasting access to the released mimetics. At the same time, the cells that were exposed to unloaded particles showed no signs of MN differentiation.

Furthermore, we demonstrated that mimetics delivered to the transplanted cells by mesoporous silica induced quick and robust differentiation of MNs in vivo after transplantation. Only transplants treated with MesoMim showed significantly improved long-term survival and extensive phenotypic MN differentiation. We found that biotinylated peptide mimetics were present at the site of transplantation for at least 10 days and associated closely with the growing neurites. The extensive growth of neurites toward the caudally located MesoMim implant suggested that the presence of a trophic gradient from this implant provided directional cues for growing neurites.

To examine whether cells in the transplants could generate neural activity, we used an optogenetic approach. Some EBs were electroporated before transplantation with a voltage-sensitive fluorescent protein, and their isolated transplants were imaged under the presence of carbachol (to promote spiking). This approach allowed the monitoring of action potentials arising from several VSFP-transfected cells without the need of patching individual neurons [10] and, to our knowledge, is the first time that a genetic reporter of the membrane potential has been used to test cell grafts for functionality. Our VSFP imaging data demonstrate that the MesoMim implants mediated the emergence of numerous electrically active and thus functional MNs in the transplants. From a technical point of view, we show that VSFP imaging not only is a valuable tool for monitoring the bulk activity of cells but also dramatically increases the success rate in localizing the transplanted cells and in registering their activity.

In summary, we have thus demonstrated that mesoporous particles allow efficient and controlled delivery of trophic factors (or their mimetics) to differentiating stem cells and can be coimplanted together with immature neural precursors to assist their final differentiation in vivo. By using this approach, we were able to reproducibly and efficiently generate functional MNs in vitro and after transplantation in vivo. Although the transplantation model was initially designed as a proof-of-principle for efficient in vivo MN differentiation, it can nevertheless already serve as a foundation for further improving stem cell-based neuroregenerative protocols.

Conclusion

Our results have clearly demonstrated that implantation of trophic factor mimetics-loaded mesoporous silica together with stem/progenitor cells is a potentially versatile approach for promoting survival as well as for efficient functional differentiation of stem cell derivatives upon transplantation.

Acknowledgments

We are grateful to Dr. Kevin Eggan for generously providing the HB9-GFP cell line; Zhanna Alekseenko, Petra Sekyrova, and Elisabet Andersson for helping establish these cultures; Rizwan Qaisar for help with confocal imaging; and Christian Berens for valuable comments on the manuscript. This work was supported by the Swedish Research Council, projects 20716 (to E.K.) and 2009-4716 (to A.E.G.-B.), Stiftelsen Olle Engkvist Byggare, and Signhild Engkvist's Stiftelse. M.K. was supported by a Visby program scholarship from the Swedish Institute. V.B., E.B., and S.P. were supported by the Lundbeck Foundation. R.L. is supported by the Kjell and Märta Beijers Foundation. A.E.G.-B. is currently affiliated with the Department of Materials and Environmental Chemistry, Stockholm University, Stockholm, Sweden.

Author Contributions

A.E.G-B.: data collection, analysis and interpretation of data, manuscript writing; M.K., C.Z., R.L., and S.P.: data collection, analysis and interpretation of data; N.K.: analysis and interpretation of data; T.K. and H.A.: analysis and interpretation of data, manuscript writing; C.T.: assembly and analysis of data; V.B. and E.B.: provision of study material, analysis and interpretation of data; E.N.K.: conception and design, manuscript writing, final approval of manuscript.

Disclosure of Potential Conflicts of Interest

E.B. and V.B. are shareholders (<0.01% shares each) in ENKAM Pharmaceuticals A/S, which owns a license to the Gliafin peptide, the patent for which is owned by Copenhagen University. A.E.G.-B. has uncompensated ownership, leadership, and cofounder roles with Nanologica AB and has uncompensated intellectual property rights as a patent holder in a related field.

References

1 Harper JM, Krishnan C, Darman JS et al. Axonal growth of embryonic stem cell-derived motoneurons in vitro and in motoneuron-injured adult rats. Proc Natl Acad Sci USA 2004; 101:7123–7128.

2 Wichterle H, Lieberam I, Porter JA et al. Directed differentiation of embryonic stem cells into motor neurons. Cell 2002;110:385–397.

3 Stacpoole SRL, Bilican B, Webber DJ et al. Efficient derivation of NPCs, spinal motor neurons and midbrain dopaminergic neurons from hESCs at 3% oxygen. Nat Protoc 2011;6:1229–1240.

4 Li XJ, Hu BY, Jones SA et al. Directed differentiation of ventral spinal progenitors and motor neurons from human embryonic stem cells by small molecules. Stem Cells 2008;26:886–893.

5 Bharali DJ, Klejbor I, Stachowiak EK et al. Organically modified silica nanoparticles: A nonviral vector for in vivo gene delivery and expression in the brain. Proc Natl Acad Sci USA 2005;102:11539–11544.

6 Vallhov H, Gabrielsson S, Stromme M et al. Mesoporous silica particles induce size dependent effects on human dendritic cells. Nano Lett 2007;7:3576–3582.

7 Garcia-Bennett AE. Synthesis, toxicology and potential of ordered mesoporous materials in nanomedicine. Nanomedicine (Lond) 2011;6:867–877.

8 Kokubo T, Kushitani H, Sakka S et al. Solutions able to reproduce in vivo surface-structure changes in bioactive glass-ceramic A-W. J Biomed Mater Res 1990;24:721–734.

9 Rønn LC, Ralets I, Hartz BP et al. A simple procedure for quantification of neurite outgrowth based on stereological principles. J Neurosci Methods 2000;100:25–32.

10 Akemann W, Mutoh H, Perron A et al. Imaging brain electric signals with genetically targeted voltage-sensitive fluorescent proteins. Nat Methods 2010;7:643–649.

11 Leão RN, Reis A, Emirandetti A et al. A voltage-sensitive dye-based assay for the identification of differentiated neurons derived from embryonic neural stem cell cultures. PLoS One 2010;5:e13833.

12 Zurn AD, Winkel L, Menoud A et al. Combined effects of GDNF, BDNF, and CNTF on motoneuron differentiation in vitro. J Neurosci Res 1996;44:133–141.

13 Rakowicz WP, Staples CS, Milbrandt J et al. Glial cell line-derived neurotrophic factor promotes the survival of early postnatal spinal motor neurons in the lateral and medial motor

columns in slice culture. J Neuro Sci 2002;22: 3953–3962.

14 Rathje M, Pankratova S, Nielsen J et al. A peptide derived from the CD loop-D helix region of ciliary neurotrophic factor (CNTF) induces neuronal differentiation and survival through binding to the leukemia inhibitory factor (LIF) receptor and the common cytokine receptor chain gp130. Eur J Cell Biol 2011;90:990–999.

15 Nielsen J, Gotfryd K, Li S et al. Role of glial cell line-derived neurotrophic factor (GDNF)-neural cell adhesion molecule (NCAM) interactions in induction of neurite outgrowth and identification of a binding site for NCAM in the heel region of GDNF. J Neurosci 2009;29: 11360–11376.

16 Levinsson A, Holmberg H, Schouenborg J et al. Functional connections are established in the deafferented rat spinal cord by peripherally transplanted human embryonic sensory neurons. Eur J Neurosci 2000;12:3589–3595.

17 Aldskogius H, Berens C, Kanaykina N et al. Regulation of boundary cap neural crest stem cell differentiation after transplantation. Stem Cells 2009;27:1592–1603.

18 König N, Akesson E, Telorack M et al. Forced Runx1 expression in human neural stem/progenitor cells transplanted to the rat dorsal root ganglion cavity results in extensive axonal growth specifically from spinal cord-derived neurospheres. Stem Cells Dev 2011;20:1847–1857.

19 Knöpfel T. Genetically encoded optical indicators for the analysis of neuronal circuits. Nat Rev Neurosci 2012;13:687–700.

20 Santos T, Maia J, Agasse F et al. Nanomedicine boosts neurogenesis: New strategies for brain repair. Integr Biol (Camb) 2012;4: 973–981.

21 Vallhov H, Kupferschmidt N, Gabrielsson S et al. Adjuvant properties of mesoporous silica particles tune the development of effector T cells. Small 2012;8:2116–2124.

22 Lu J, Liong M, Li Z et al. Biocompatibility, biodistribution, and drug-delivery efficiency of mesoporous silica nanoparticles for cancer therapy in animals. Small 2010;6:1794–1805.

23 Hudson SP, Padera RF, Langer R et al. The biocompatibility of mesoporous silicates. Biomaterials 2008;29:4045–4055.

24 Witasp E, Kupferschmidt N, Bengtsson L et al. Efficient internalization of mesoporous silica particles of different sizes by primary human macrophages without impairment of macrophage clearance of apoptotic or antibody-opsonized target cells. Toxicol Appl Pharmacol 2009;239:306–319.

See www.StemCellsTM.com for supporting information available online.